Article:
Lai, X, Jiang, H and Wignall, PB (2018) A review of the Late Permian – Early Triassic conodont record and its significance for the end-Permian mass extinction. Revue de Micropaleontologie, 61 (3-4). pp. 155-164. ISSN 0035-1598

https://doi.org/10.1016/j.revmic.2018.10.002

A review of the Late Permien - Early Triassic conodont record and its significance for the end Permian mass extinction

Xulong Lai[1,2*], Haishui Jiang[1,2] , Paul B.Wignall[3]

1. School of Earth Science, China University of Geosciences, Wuhan, Hubei 430074, P.R.China

2. State Key Laboratory of Biogeology and Environmental Geology, China University of Geosciences, Wuhan, Hubei 430074, P.R.China

3. School of Earth & Environment, University of Leeds, Leeds, LS2 9JT, UK

Abstract

As one kind of marine microfossil lasted from Cambrian to Triassic, the tiny conodont plays an important role for the studying the end-Permian mass extinction. In past decades, numberous of works on Permian-Triassic conodonts have been published. This paper mainly deals with the progresses on high-resolution conodont biostratigraphy, timing of the mass extinction across the Permian-Triassic Boundary, conodont apparatus and phylogeny, conodont size variation, conodont oxygen isotope as well as other isotopes and chemical elements. Finally, perspectives in future works is also made.

Keywords

Conodont, Permian-Triassic , biostratigraphy, palaeoenvironment, end-Permian mass extinction

1. Introduction

The end-Permian mass extinction was the largest crisis in the geological history. It devastated the Paleozoic ecosystem and led to the disappearance of more than 90% marine species and 70% of terrestrial vertebrates in the land (e.g. Erwin, 1993; Hallam and Wignall, 1997; Payne and Clapham, 2012). Conodonts were one of few marine taxa to survive throughout the end-Permian mass extinction relatively unscathed. Due to its fast evolutionary rates , conodont plays an important role in the study of biostratigraphy and chronostratigraphy of the entire Permian and Triassic interval.

Since Yin et al. (1988) proposed the first appearance of conodont species *Hindeodus parvus* (Kozur and Pjatakova, 1976) as a marker for the base of the Triassic, the study of the conodont faunas across the P/T boundary has received much attention with many studies of. conodont diagnosis, zonation, regional and global correlation, clines and biofacies in last

century.Although the Global Stratotype Section and Point (GSSP) of the Permian- Triassic Boundary was ratified at the Meishan section, Zhejiang Province, South China in 2001（Yin et al., 2001）, conodonts are still intensively studied because it plays a key role on understanding the biotic evolution and environmental as well as climatic changes during the Permian-Triassic transitional period. For better understanding the progresses on P/T conodont study, in this paper, we mainly review the major progresses on P/T conodont studies since 2001 especially in past decade. Perspectives in future works is also made.

2. Biostratigraphy and timing of the mass extinction across the Permian-Triassic Boundary (PTB)

2.1 Conodont biostratigraphy

Key conodont species (Fig. 1) play very important roles in defining the biostratigraphy across the PTB since the first appearance of *Hindeodus parvus* has been proposed as the marker for the base of Triassic System (Yin et al., 1988). For decades, numerous conodont studies of the Meishan section, the Global Stratotype Section and Point (GSSP) for the PTB (Yin et al., 2001) have been undertaken (e.g. Wang and Wang (1981), Zhang (1984, 1987), Wang (1994, 1995a, 1995b, 1996), Zhang et al. (1995, 2009), Lai et al. (1995, 2001), Mei et al. (1998), Jiang et al. (2007, 2008, 2011a, 2011b), Yuan et al. (2014). These works have produced a high-resolution conodont zones across the PTB at Meishan section, which was summarized by Zhang et al. (2009), Yin et al. (2014) and Chen Z.Q. et al. (2015).

Besides the Meishan section, conodont biostratigraphy across the PTB have also been well studied at numerous sections in southern China, e.g. Chaohu section in Anhui (Zhao et al., 2007); Shangsi section (Nicoll et al., 2002; Jiang et al., 2011b) and Chaotian section (Isozaki et al., 2003; Ji et al., 2007) in Sichuan; Liangfengya section (Yuan et al., 2011) and Dajiagou section (Yuan et al., 2015) in Chongqing; Huangsi Ermen section (Wang and Xia, 2003), Xiakou section (Wang and Xia, 2004), Daxiakou section (Zhao et al., 2013) and Jianzishan section (Bai et al., 2017) in Hubei; Cili section in Hunan (Wang et al., 2016); Dongpan section (Luo et al., 2008) and Wuzhuan section (Brosse et al., 2015) in Guangxi; Huangzhishan section (Chen et al., 2008; Chen et al., 2009) in Zhejiang; Xinfeng Tieshikou section(Wu et al, 2003), Yangou section in Jiangxi (Wu et al., 2002; Sun D.Y. et al., 2012); Gaimao section (Yang et al., 2012), Bianyang section (Yan et al., 2013; Jiang et al., 2015), Xinmin section (Zhang et al., 2014), Dawen section (Chen et al., 2009b), Dajiang section (Jiang et al., 2014) , Jiarong section (Chen Y.L. et al., 2015) , Mingtang section (Liang et al.,

2016) and Zhongzhai section (Metcalfe and Nicoll, 2007) in Guizhou; Selong section (Wang et al., 2017; Yuan et al., 2018), Wenbudangsang section (Wu et al., 2014) in Tibet.

Outside of South China, as well as, conodont biostratigraphy across the PTB have been studied in the Southern Alps (Perri and Farabegoli, 2003); Iran (Kozur, 2007; Yousefirad, 2013; Chaderi et al., 2014); Guryul Ravine section in India (Brosse et al., 2017); Lung Cam section (Wardlaw et al., 2015), Son La section (Metcalfe, 2012) in Vietnam; Lukac section in Slovenia (Kolar-Jurkovsek et al., 2011); Bükk Moutain section in Hungary (Sudar et al., 2008); Komiric section in northwestern Serbia (Sudar et al., 2007); Chitral section in northernmost Pakitan (Perri et al., 2004); Marble Range in South-Central British Columbia (Beyers and Orchard, 1991); Montney Formation in the Peace River Basin from west-central Alberta to east-central British Columbia(Henderson et al., 2018); Central British Columbia area (Orchard et al., 1998); Arctic Canada (Henderson and Baud, 1996； Algeo et al., 2012); Kamura section in southern Japan (Zhang et al., 2017).

Globally, conodont sequences across the PTB are best known from the Tethys region. Here we summarized the Tethyan conodont zones across the PTB established using lineages of gondolellids and hindeodids.

2.1.1. Gondolellid zonation

In ascending order, the gondolellid zones are discussed as follows (Fig. 2):

Clarkina changxingensis Zone: Lower limit: the first appearance datum (FAD) of *C. changxingensis*, upper limit: the FAD of *C. yini*. This zone is reported at Meishan (Yuan et al., 2014), Yangou (Sun D.Y. et al., 2012), Spiti (Orachrd & Krystyn, 1998), and correlated with the *C. changxingensis- C.deflecta* assemblage zone in Iran. The *C. changxingensis* Zone is contemporaneous with the *Hindeodus latidentatus* Zone and *H. julfensis* Zone (Fig. 2).

Clarkina yini Zone: Lower limit: the FAD of *C. yini*, upper limit: the FAD of *C. meishanensis*. This zone is reported at Meishan (Jiang et al., 2007; Yuan et al., 2014), Shangsi (Jiang et al., 2011b), Xinmin (Zhang et al., 2014), Yangou (Sun D.Y. et al., 2012), and may include the *C. zhangi* Zone of Iran (Kozur, 2007) (Fig. 2). The *C. yini* Zone may also correlate to the Lower *H. praeparvus* zone (Fig. 2).

Clarkina meishanensis Zone: Lower limit: the FAD of *C. meishanensis*, upper limit: the FAD of *C. taylorae*. This zone is reported at Meishan (Jiang et al., 2007; Yuan et al., 2014), Shangsi (Jiang et al., 2011b), Xinmin (Zhang et al., 2014), and correlated to the *C. meishanensis- H. praeparvus* assemblage zone in Iran (Fig. 2).

Clarkina taylorae Zone: Lower limit: the FAD of *C. taylorae*, upper limit: the FAD of *C. planata*. This zone is reported at Meishan (Jiang et al., 2007), Shangsi (Jiang et al., 2011b), Yangou (Sun D.Y. et al., 2012), and may correlate with the upper *H. changxingensis* Zone in South China, or the top of *H. praeparvus* Zone in Spiti and Southern Alps (Fig. 2).

Clarkina planata Zone: Lower limit: the FAD of *C. planata*, upper limit: the FAD of *C. krystyni*. This zone is reported at Meishan (Zhang et al., 2009) and Gaimao (Yang et al., 2012), where it occurs above the *Isarcicella isarcica* Zone. However, the FAD of *C. planata* coincides with the FAD of *H. parvus* at Spiti (Orachrd & Krystyn, 1998) and so is present at a lower level. The higher 'FAD' of *C. planata* at Meishan and Gaimao may due to facies control at these locations..

Clarkina krystyni Zone: Lower limit: the FAD of *C. krystyni*, upper limit: the FAD of *Neoclarkina discreta*. This zone is reported at Chaohu (Zhao et al., 2007), Gaimao (Yang et al., 2012), Jiarong (Chen Y.L. et al., 2015) and Spiti (Orachrd & Krystyn, 1998). This zone may correlate with the upper *I. staeschei* Zone, *I. isarcica* Zone and *H. sosioensis* Zone (Fig. 2). The higher 'FAD' of *C. krystyni* at Gaimao (Yang et al., 2012) and Jiarong (Chen Y.L. et al., 2015) may also due to facies controls.

Neoclarkina discreta Zone: Lower limit: the FAD of *Nc. discreta*, upper limit: the FAD of *Sweetospathodus kummeli*. This zone is reported at Meishan (Chen Z.Q. et al., 2015), Jiarong (Chen Y.L. et al., 2015), Mingtang (Liang et al., 2016) and Spiti (Orachrd & Krystyn, 1998). This zone may be the last gondolellid conodont zone of the Griesbachian.

2.1.2. Hindeodid zonation

In ascending order, the Permian-Triassic hindeodid zones are as follows (Fig. 2):

Hindeodus latidentatus Zone: Lower limit: the FAD of *H. latidentatus*, upper limit: the FAD of *H. praeparvus*. This zone is reported at Meishan (Jiang et al., 2007) and Spiti (Orachrd & Krystyn, 1998). However, the *H. latidentatus* Zone at Spiti may correlate to the *C. changxingensis* Zone and *C. yini* Zone. But the *H. latidentatus* Zone at Meishan may only correlate with the top of the *C. changxingensis* Zone (Fig. 2).

Hindeodus praeparvus Zone: Lower limit: the FAD of *H. praeparvus*, upper limit: the FAD of *H. changxingensis*. This zone is reported at Meishan (Jiang et al., 2007), Spiti (Orachrd & Krystyn, 1998), Southern Alps (Perri & Farabegoli, 2003) and Iran (Kozur, 2007). It correlates with the *C. yini* Zone and the upper *C. meishanensis* Zone (Fig. 2).

Hindeodus changxingensis Zone: Lower limit: the FAD of *H. changxingensis*, upper limit: the FAD of *H. parvus*. This zone is reported at Meishan (Jiang et al., 2007), Shangsi (Jiang et

al., 2011b), Xinmin (Zhang et al., 2014), and Yangou (Sun D.Y. et al., 2012). It correlates with the upper *C. meishanensis* Zone and *C. taylorae* Zone (Fig. 2).

Hindeodus parvus Zone: Lower limit: the FAD of *H. parvus*, upper limit: the FAD of *I. lobata*. This zone is widely reported including fromMeishan (Jiang et al., 2007), Shangsi (Jiang et al., 2011b), Dajiang (Jiang et al., 2014), Xinmin (Zhang et al., 2014), and Yangou (Sun D.Y. et al., 2012), Jiarong (Chen Y. L. et al., 2015), Spiti (Orachrd & Krystyn, 1998), Southern Alps (Perri & Farabegoli, 2003), Iran (Kozur, 2007) , North America (Algeo et al., 2012; Beyers and Orchard 1991, Henderson and Baud 1996) and other sections in the world. The FAD of *H. parvus* marks the base of Triassic System (Yin et al, 2001).

Isarcicella lobata Zone: Lower limit: the FAD of *I. lobata*, upper limit: the FAD of *I. staeschei*. This zone is reported from Shangsi (Jiang et al., 2011b), Dajiang (Jiang et al., 2014) and Southern Alps (Perri & Farabegoli, 2003) (Fig. 2).

Isarcicella staeschei Zone: Lower limit: the FAD of *I. staeschei*, upper limit: the FAD of *I. isarcica*. This zone is reported from Meishan (Jiang et al., 2007), Yangou (Sun D.Y. et al., 2012), Spiti (Orachrd & Krystyn, 1998) and Southern Alps (Perri and Farabegoli, 2003) (Fig. 2).

Isarcicella isarcica Zone: Lower limit: the FAD of *I. isarcica*, upper limit: the FAD of *H. sosioensis*. This zone is reported from Meishan (Jiang et al., 2007), Shangsi (Jiang et al., 2011b), Dajiang (Jiang et al., 2014), Yangou (Sun D.Y. et al., 2012), Gaimao (Yang et al., 2012), Southern Alps (Perri and Farabegoli, 2003), Iran (Kozur, 2007), and may correlate to the lower *H. postparvus- I. isarcica* assemblage zone at Spiti (Orachrd & Krystyn, 1998) (Fig. 2).

Hindeodus sosioensis Zone: Lower limit: the FAD of *H. sosioensis*, upper limit: uncertain. This zone is reported at Wadi Wasit (Oman, Krystyn et al., 2003), Dajiang (Jiang et al., 2014), Jiarong (Chen Y. L. et al., 2015), and may correlate to the top of *C. krystyni* Zone (Fig. 2).

2.2 Discussion:

Zhang et al. (2014) reported *H. parvus* from bed 28 at the Zhongzhai section, Guizhou, but they put the PTB at the base of bed 30, which is 18 cm higher than the FAD of *H. parvus*, mainly because of the significant negative shift of carbonate carbon isotopes at this level. They surmised that the first occurrence (FO) of *H. parvus* is diachronous but, we considered that the PTB at the Zhongzhai section should be placed at the horizon of the base of bed 28. Using this lower level implies that there has been possible contamination, reworking of Permian faunas or a delayed extinction (e.g. Jiang et al., 2015) at the Zhongzhai section.

Recently, the use of conodont Unitary Associations Zones (UAZs) has triggered discussions of the biostratigraphy of the PTB (Brosse et al., 2016; Jiang et al., 2017; Brosse et al., 2017). But as stated in Jiang et al. (2017), the UAZs method 'does not provide an improvement on the use of conventional interval zones in the PTB interval'. Ellwood et al. (2017) used a graphic correlation method to identify a globally synchronous PTB timescale but assumed the FO of *H. parvus* was diachronous due to slow dispersal or migration of this species. However, the graphic correlation method requires needs a globally synchronous signal to be applied. Ellwood et al. (2017) assumed the extinction event level (and the ash bed seen in South China) are coeval. However, there is an abundant literature that demonstrates the PTB extinction losses are diachronous and do not constitute a short-lived event (e.g. Wignall & Newton, 2003; Song et al., 2013; Grasby et al., 2015). Correlating using high-resolution conodont biostratigraphy shows the mass extinctions in deep-water locations such as Bianyang and Shangsi is delayed (Jiang et al., 2015), whilst the two ash beds near the PTB at the Meishan section (see to Yin et al., 2001) cannot correlate with the six ash beds near the PTB at the Shangsi section (see Nicoll et al., 2002). So, the supposedly globally synchronous proxies selected Ellwood et al. (2017) are, at best, questionable.

Although two detailed conodont zones across the PTB in two different lineages of gondolellids and hindeodids can be summarized globally, the interval zones defined by the FAD of some species (without considering their lineage context) is often used in correlation (e.g. Yin et al., 2014). The high-resolution conodont biostratigraphy provided a detailed time coordinate to study the geological events during the PTB. Yin et al. (2014) found that the Yangtze and other isolated carbonate platforms in South China experienced sedimentary hiatus during the *C. meishanensis* Zone and *H. changxingensis* Zone.

2.3 Timing of the PTB mass extinction

The patterns and timing of the mass extinction across the PTB have been intensively studied for decades. Many of these studies have focused on sections of South China, especially the Meishan section. Jin et al. (2000) studied the genera and species across the PTB at the Meishan type section. Their results show a sharp extinction coincident with a dramatic negative shift of $\delta^{13}C_{carb}$ curve at the base of bed 25, correlated to the base of *C. meishanensis* Zone (Fig. 3, A). Later, Xie et al. (2005) found two episodes associated with microbial change across the PTB at the Meishan section,. These occurred at the base of bed 25 and the base of bed 28, correlated to the base of *C. meishanensis* Zone (Fig. 3, B1) and the base of *I. staeschei* Zone (Fig. 3, B2), respectively. Yin et al. (2007) re-studied the fossils and events at the Meishan PTB section and found that the PTB mass extinction has a more

complicated pattern, consisting of a prelude, main episode and epilogue, at the base of bed 24e, during beds 25-26 and at the bed 28 respectively. These correlate with the base of *C. meishanensis* Zone (Fig. 3, C1), *C. meishanensis* Zone to *H. changxingensis* Zone (Fig. 3, C2) and the base of *I. staeschei* Zone (Fig. 3, C3). The PTB mass extinction was reassessed once again by Shen et al. (2011) and essentially replicated the conclusion of Yin et al. (2007): the mass extinction interval was seen to start at the base of bed 24e and end in bed 28 of Meishan (Fig. 3, D). The problem with all these studies is that they only considered the extinction record at a single section, Meishan. Song et al. (2013) studied seven PTB sections from a spectrum of water depths in South China and documented the range of 537 species to the level of conodont zones. This demonstrated two extinction pulses during the PTB, one in the latest Permian extinction, another is the earliest Triassic extinction, occurred at the base of *C. meishanensis* Zone (Fig. 3, E1) and in *I. staeschei* Zone (Fig. 3, E2), respectively. Recently, Jiang et al. (2015) studied the conodonts and foraminifers at the deep-water Bianyang PTB section, and found a delayed onset of extinction, beginning at the base of *H. parvus* Zone, (Fig. 3, F). According to the level of the negative $\delta^{13}C_{carb}$ excursion at Shangsi, Jiang et al. (2015) showed that the PTB mass extinction of this section may occurred at the base of *C. taylorae* Zone (Fig. 3, G).

Thus, there is a prolonged extinction interval during the PTB transition that ranges from the top part of *C. yini* Zone to the *I. staeschei* Zone (Fig. 3). This interval coincides with a major warming phase that is likely to have played an important role in the mass extinction (Sun et al., 2012; Joachimski et al., 2012; Jiang et al., 2015). The 8~10 ºC global warming happened in almost 60,000 years, although temporal resolutuoon is insufficient to judge of the pace of warming was uniform or variable. .

3. Reconstruction of apparatus and phylogeny of PTB conodonts

3.1 Reconstruction of Apparatuses

The genus *Clarkina* is common in the PTB interval. Based on the apparatus plate of the Middle Triassic species *Neogondolella momberensis*, Orchard & Rieber (1999) restored a fifteen element apparatus of the Late Permian species *Neogonodolella* (=*Clarkina*) *subcarinata,* including an unpaired Sa element, and paired Pa elements, Pb elements, M elements, Sb1 elements, Sb2 elements, Sc1 elements and Sc2 elements. All complete apparatuses of superfamily Gondolelloidea of Triassic are now regarded as consisting of 15 elements (Orchard, 2005). Huang et al. (2010, 2018) found numerous conodont clusters in Guanling Formation from the Daaozi section at Luoping, the location with Luoping Biota,

Yunnan, South China. Based on those clusters, they restored a conodont multi-element apparatus although without given a name for it. Goudemand et al. (2012) investigated the clusters from the Early Triassic strata at Youping, Waili and Zuodeng of Guangxi. They shifted the positions of previous S1 and S2 elements of superfamily Gondolelloidea. Additionally, they also shifted the positions of previous S3 and S4 elements of subfamily Novispathodinae.

Hindeodid conodonts, including *Hindeodus* and *Isarcicella*, with very similar apparatuses (e.g. Jiang et al., 2011a), are also common and important during PTB. Based on the collection of 13 assemblages from lowermost Triassic strata in the Mino Terrane, Japan, Agematsu et al. (2014) restored the apparatuses *Hindeodus parvus* and *Hindeodus typicalis*, and suggested they both consist of 15 elements although their examples comprised at most 13 elements. Later, Agematsu et al. (2017) demonstrated that genus *Hindeodus* had a 15 elements apparatus by finding the S1 elements under the synchrotron radiation micro-tomography (SR–μCT). At the same time, according to the six hindeodid clusters obtained from lowermost Triassic strata in the Shangsi, South China reported by Jiang et al. (2011) and the assemblages of Agematsu et al. (2014), Zhang et al. (2017) suggested that *Hindeodus parvus* probably had 13 elements: unpaired S0 element; symmetrically paired S1, S2, S3, S4 and P1 elements, but no P2 elements. Some Triassic conodonts may therefore have had a reduced dentition (see Agematsu et al., 2018; Purnell et al., 2018), although other studies suggest otherwise.

A natural assemblage of *Ellisonia* sp. cf. *E. triassica* Müller was reported from the uppermost Permian in the Suzuka Mountains, central Japan (Koike et al., 2004). Although there were only 11 elements in their assemblage, they still interpreted genus *Ellisonia* had a standard 15 elements apparatus. The species *Hadrodontina aequabilis* was reported in *I. staeschei* Zone and *I. isacica* Zone (Perri and Farabegoli, 2003). Some fused clusters from uppermost Smithian limestone of the Taho Formation, Japan, Koike (2016) have been restored with a 15 element apparatus.

3.2 Phylogeny

There have been many studies of hindeodid phylogeny (e.g. Kozur, 1989; Zhang *et al.*, 1995; Ding *et al.*, 1996; Wang, 1996; Kozur, 1996; Lai, 1998; Perri & Farabegoli, 2003; Orchard, 2007), although only Jiang et al. (2011a) have used a cladistic approach based on P1 elements of *Hindeodus* and *Isarcicella*. The resultant phylogeny did not concur entirely with those previous hypotheses (e.g. *H. parvus* was not shown to be a direct descendant of *H. praeparvus*) but, species assigned to the genus *Isarcicella* formed a natural group (Fig. 4).

The evolutionary relationships among gondolellid genera *Clarkina*, *Neoclarkina*, *Neospathodus* and *Neogondolella*, suggested by Henderson and Mei (2007), has been debated (Jiang et al., 2014). Jiang and Lai (2013) undertook cladistic analysis, based on 76 characters for 36 multielemental apparatus species, from the Pennsylvanian to the Late Triassic. Their results indicated that the genera *Clarkina*, *Neoclarkina* and *Neogondolella* were closer to each other than to *Neospathodus* and this Early Triassic genus was not resolved as evolving from *Neoclarkina*.

4. Conodont size variation during mass extinction

Urbanek (1993) used the term "Lilliput effect" for an observed size reduction of Silurian graptolites during a biotic crisis and Twitchett (2005) noted a size reduction of organisms like bivalves and brachiopods during the Permian-Triassic transition. Conodonts also seem to have responded to this crisis by reducing in size. Based on both a generic and species level investigation of the individual size of over three thousand specimens of the latest Permian conodont *Neogondolella* (*Clarkina*) P1 elements collected from beds 24a to 24e at Meishan section, Zhejiang Province. Luo et al. (2006) recognized a significant size reduction of this genus in bed 24e, a level marked by mass extinction of other taxa. Later, Luo et al. (2008) measured over one thousand of P1 elements of both genera *Hindeodus* and *Isarcicella* from bed 24a to bed 29 at Meishan section and showed a clear size reduction of these hindeodids in bed 24e.

At the Jiarong section, Guizhou province, detailed size measurements of 441 conodont elements of genera *Neospathodus*, *Triassospathodus*, and *Novispathodus* show these genera suffered a temporary, but significant size reduction during the Early Triassic Smithian-Spathian Boundary crisis. This size reduction of conodonts was coincided with peak hot temperature of this interval revealed by the conodont oxygen isotope analysis (Chen et al, 2013).

By comparing Permian-Triassic body size trends globally in eight marine clades including conodonts, Schaal et al. (2016) measured over 10 thousands specimens and 2,743 species spanning the Late Permian through the Middle to Late Triassic. This work indicated out the Permian/Triassic boundary (PTB) shows more size reduction among species than any other interval.

Above studies confirmed that conodont is a taxon sensitive to the palaeoenvironmental and climatic changes.

5. Conodont geochemistry

Conodont elements are composed of carbonate-fluorapatite, a mineralogy that has proved a useful record of many chemical and istopic attributes of the sea water from which it formed. The successful survival of many conodont species during the mass extinction further ensures the unrivalled importance of conodonts for the study of environmental and geochemical changes during the crisis.

5.1 Conodont oxygen isotope

The oxygen isotopes ratio of phosphate-bound oxygen of conodont apatite has been shown to be relatively immune to diagenetic alteration and thus has been a valuable tool for reconstructing paleoclimate changes (e.g. Joachimski et al., 2009). Based on chemical dissolution method, Joachimski et al. (2012) studied the studied conodont oxygen isotopes from Meishan and Shangsi PTB that revealed a decrease of 2 ‰ in the latest Permian. This translates into a surface sea water warming of 8º (Fig. 3). Based on an analysis of conodont oxygen isotopes from five sections in the Nanpanjiang basin, South China, Sun et al. (2012) revealed the very warm sea-surface temperatures persisted into the Early Triassic, with two temperature peak at late Griesbachian and late Smithian (up to 41º), and suggested that the extreme temperatures delayed the recovery of the Early Triassic ecosystems. In Palaeotethys, Schobben et al. (2014) also reported a major temperature rise during late Permian following the end-Permian mass extinction in northwestern Iran.

The phosphate dissolution approach gives reliable results but it requires large samples: about 0.5 mg of conodont samples which is equivalent to several tens of gondolellids or over one hundred *Neospathodus* conodont specimens. In contrast, SHIRMP analysis allows single elements to be targeted using high-resolution SIMS and GIMS and so has been widely used in PTB and Triassic studies (e.g. Zhou et al., 2012; Trotter et al., 2015; Chen et al., 2016).However, work is ongoing to improve the techniques (e.g. Griffin et al., 2015; Quinton et al., 2016; Sun et al., 2016; Mine et al., 2017).

5.2 Other isotopes and elements from conodont

The significant changes in seawater $^{87}Sr/^{86}Sr$ values during the P/T transition were initially based on whole rock analysis of carbonate samples and brachiopod shells (e.g. Hosler and Magaritz, 1987, Gruszczynski et al., 1992). The first use of conodont apatite for Sr isotope analysis was attempted by Martin and Macdougall (1995). Using LA-MC-ICPMS technique, Song et al. (2015) measured $^{87}Sr/^{86}Sr$ data of 127 conodont samples collected from

several sections in South China, and recognized a rapid rise of $^{87}Sr/^{86}Sr$, beginning in Bed 25 of the Meishan section, and coinciding closely with mass extinction (Song et al., 2015), although the more recent study of Dudas et al. (2017) concluded that the rapid rise in seawater $^{87}Sr/^{86}Sr$ began at least 30 kyr prior to the onset of marine extinction at Meishan.

The marine calcium isotope system has also been investigated using PTB conodont apatite (Hinojosa et al., 2012; Le Houedec et al. 2017), The $\delta^{44}Ca/^{40}Ca$ record shows a negative excursion similar in stratigraphic position and magnitude to that previously observed in carbonate rocks.

During past years, other chemical constituents PTB conodont apatite have received study (e.g. Zhao et al, 2009, 2013; Chen et al., 2012; Katvala et al., 2012; Song et al., 2012; Li et al., 2017 etc.). Using a LA-ICP-MS technique, Zhao et al. (2009) measured the trace element compositions in Upper Permian conodonts at Meishan section to show rapid fluctuations of Ce anomalies and rare earth element (REE) . The Ce anomaly and variation of Th/U have also revealed redox fluctuations during the extinction interval (Song et al. 2012), whilst REE patterns in conodont have been ascribed to explosive volcanism during the crisis (Zhao et al., 2013).

6. Perspectives

6.1 . High-resolution conodont biostratigraphy

High-resolution conodont biostratigraphic works have provided a reliable and precise time framework for the study of biotic and environmental events during the P/T transition, but it remains an important field of P/T conodont study. For example, conodont occurrences from higher palaeolatitude areas are relatively poorly understood, and studies are required to help better understand the evolution of this group. Also, most investigations of P/T conodonts have been made in carbonate-dominated, shallow water palaeoenvironments and more work is needed from deep-water sections.

6.2. Conodont taxonomy

Conodont taxonomy fundamentally underpins biostratigraphy. Although there are only few major conodont genera (*Clarkina* (*Neogondolella*)*, Neoclarkina, Hindeodus, Isarcicella*) in the P/T transition interval, there were several tens of species. Sometimes, many species of the same genus can be reported from same sample in some previously published data. For defining the base of the Changhsingian Stage, Lopingian Series, Upper Permian，Henderson et al. (2014) proposed the sample-population based taxonomic approach. This

approach usually views the entire collection within a given sample as a population and recognizes the most consistent and stable characters within that 'sample-population' for identification. This approach may avoid misidentification of specimens belonging to different ontogenic stages into different species. Unfortunately, there were few conodont workers followed this approach. It might be caused by the species established by sample population approach with wide range of morphological variation, and it is not easily to distinguish the inter-species and intra-species characters. It is more difficult to use sample population approach than use the traditional morphological method (holotype) during the conodont identification. Combining the sample population approach concept with morphometric methodology, to investigate both the ontogeny and phylogeny of different clades, can help evaluate the validity of established species.

6.3. Conodont clusters and natural assemblages

Only a few natural assemblages and clusters have been reported from the P/T intervals, although the situation has improved in the past few years. This is because conodont workers are paying more attention to finding conodont apparatuses. It is to be hoped that more and more conodont clusters, natural assemblages and even soft body will be found in future.

6.4. Conodont palaeoecology and microwears

Palaeoecology of P/T conodont has received little study in recent years. Besides functional morphology, conodont microwear analysis can provide evidence of both diet and feeding kinematics that is independent of morphological analysis (Purnell and Jones, 2012). It has yet to be seen if conodont microwear changed during the mass extinction. Findings may provide clues to the successful survival of this group in the stressed environments of the P/T transitional period.

6.5. Conodont geochemistry

Conodont apatite will no doubt remain a favourite material for geochemical study of the palaeoenvironmental and climatic changes during the P/T transitional period. As the techniques improving, and geochemists and conodont workers closely work together, it is expected there will be more and more results or surprises from conodont geochemical studies. For apatite oxygen isotope analysis, most work has focused on low-latitude Tethyan regions. More data from other regions like Perigondwana and other high palaeolatitude areas would allow us to compare the temperature difference between different regions, and better understand the global climatic system in P/T transition.

Acknowledgement

This study is supported the Natural Science Foundation of China (grants No. 41572002, 4172324, 41272044, 41661134047). The authors greatly appreciate professor Maicheal Joachimski, the long-term collaboration with him widely broaden our knowledge to conodont apatite oxyegen isotopes and its implication to the.end-Permian mass extinction. Thanks also due to Doctors Yadong Sun, Yanlong Chen, Lina Wang, Muhui Zhang for valuable discussion with them during past years. We thank Doctors Martyn Golding, Pablo Plasencia，Taniel Danelian and other two anonymous reviewers for their helpful comments and constructive suggestions.

References

Agematsu, S., Sano, H. and Sashida, K. 2014. Natural assemblages of Hindeodus conodonts from a Permian–Triassic boundary sequence, Japan. Palaeontology, 57: 1277–1289.

Agematsu, S., Uesugi, K., Sano, H., Sashida, K., 2017. Reconstruction of the multielement apparatus of the earliest Triassic conodont, Hindeodus parvus, using synchrotron radiation X-ray micro-tomography. Journal of Paleontology, 91(6): 1220–1227.

Agematsu, S., Golding, M.L. and Orchard, M.J., 2018. Comments on: testing hypotheses of element loss and instability in the apparatus composition of complex conodonts (Zhang et al.). Palaeontology doi: 10.1111/pala.12372.

Algeo, T., Henderson, C.M., Ellwood, B., Rowe, H., Elswick, E., Bates, S., Lyons, T., Hower, J.C., Smith, C., Maynard, B., Hays, L.E., Summons, R.E., Fulton, J., and Freeman, K.H., 2012. Evidence for a diachronous Late Permian marine crisis from the Canadian Arctic region. Geological Society of America Bulletin, 124:1424-1448.

Bai, R.Y., Dai, X., Song, H.J. 2017. Conodont and ammonoid biostratigraphies around the Permian-Triassic Boundary from the Jianzishan of South China. Journal of Earth Science, 28: 595-613.

Beyers, J.M. and Orchard, M.J., 1991. Upper Permian and Triassic conodont faunas from the type area of the Cache Creek Complex, south-central British Columbia, Canada. Geological Survey of Canada Bulletin, 417: 269-297.

Brosse, M., Bucher, H., Bagherpour, B., Baud, A., Frisk, Å. M., Guodun, K., Goudemand, N., 2015. Conodonts from the Early Triassic microbialite of Guangxi (South China): Implication for the definition of the base of the Triassic system. Palaeontology, 58:563-584.

Brosse, M., Bucher, H., Goudemand, N., 2016. Quantitative biochronology of the Permian–Triassic boundary in South China based on conodont Unitary Associations. Earth-Science Reviews, 155: 153–171.

Brosse, M., Bucher, H. and Goudemand, N., 2017. Reply to the Comment on "Quantitativ biochronology of the Permian-Triassic boundary in South China based on conodont unitary associations." Earth-Science Reviews, 164: 259-261.

Brosse,M., Baud, A., Bhat, G.M., Bucher, H., Leu, M., Vennemann, T., Goudemand, N., 2017. Conodont-based Griesbachian biochronology of the Guryul Ravine section (basal Triassic, Kashmir, India). Geobios, 50(5-6): 359-387.

Burgess, S.D., Bowring, S., Shen, S.Z., 2014. High-precision timeline for Earth's most severe extinction. Proc. Natl. Acad. Sci. U. S. A. 111 (9): 3316–3321.

Chen, J., Henderson, C.M. and Shen, S. Z., 2008, Conodont succession around the Permian–Triassic boundary at the Huangzhishan section, Zhejiang and its stratigraphic correlation. Acta Palaeontologica Sinica 47: 91–104.

Chen, J., Beatty, T. W., Henderson, C. M. and Rowe, H., 2009, Conodont biostratigraphy across the Permian–Triassic boundary at the Dawen section, Great Bank of Guizhou, Guizhou Province, South China: Implications for the Late Permian extinction and correlation with Meishan. Journal of Asian Earth Sciences 36: 442–458.

Chen, J., Shen, S.Z., Li, X.H., Xu, Y.G., Joachimski, M.M., Bowring, S.A., Erwin, D.H., Yuan, D.X., Chen, B., Zhang, H., Wang, Y., Cao, C.Q., Zheng, Q.F., Mu, L., 2016. High-resolution SIMS oxygen

isotope analysis on conodont apatite from South China and implications for the end-Permian mass extinction. Palaeogeography Palaeoclimatology Palaeoecolog, 448: 26-38.
Chen, J.B., Zhao, L.S., Chen, Z.Q., Tong, J.N., Zhou, L., Hu, Z.C., Chen, Y.L., 2012. In Situ Rare Earth Elements in Conodont from Meishan Section in Zhejiang Province and Implications for Paleoenvironmental Evolution. Earth Science, 37: 25-34. (In Chinese with English summary)
Chen, Y.L, Jiang, H.S., Lai, X.L., Yan, C.B., Richoz, S., Liu, X.D., Wang, L.N., 2015, Early Triassic conodonts of Jarong, Nanpanjiang basin, southern Guizhou Province, South China. Journal of Asian Earth Sciences 105: 104–121.
Chen Z.Q., Yang H, Luo M, Benton M J, Kaiho H, Zhao L S, Huang Y G, Zhang K X, Fang Y H, Jiang H S, Qiu H, Li Y, Tu C Y, Shi L, Zhang L, Feng X Q, Chen L, 2015. Complete biotic and sedimentary records of the Permian–Triassic transition from Meishan section, South China: Ecologically assessing mass extinction and its aftermath. Earth-Science Reviews 149: 63–103.
Clark, D.L., 1959. Conodonts from the Triassic of Nevada and Utah. Journal of Paleontology, 33(2): 305-312.
Ding, M.H., Zhang, K.X., Lai, X.L., 1996. Evolution of Neogondolella lineage and *Hindeodus–Isarcicella* lineage at Meishan section, South China. In Yin, H.F. (ed.): The Palaeozoic–Mesozoic Boundary, Candidates of the Global Stratotype Section and Point of the Permian–Triassic Boundary, 65–71. China University of Geosciences Press, Wuhan.
Dudas, F.O., Yuan, D.X., Shen, S.Z., Bowring, S.A., 2017. A conodont-based revision of the Sr-87/Sr-86 seawater curve across the Permian-Triassic boundary. Palaeogeography Palaeoclimatology Palaeoecology,470: 45-53.
Ellwood, B.B., Wardlaw, B.R., Nestell, M.K.., Nestell, G.P., Lan, L.T.P., 2017. Identifying globally synchronous Permian–Triassic boundary levels in successions in China and Vietnam using Graphic Correlation. Palaeogeography Palaeoclimatology Palaeoecology, 485: 561-571.
Erwin, D.H., 1993. The Great Paleozoic Crisis: Life and Death in the Permian. CU Press.
Ghaderi, A., Leda, L., Schobben, M., Korn, D., Ashouri, A.R., 2014. High-resolution stratigraphy of the Changhsingian (Late Permian) successions of NW Iran and the Transcaucasus based on lithological features, conodonts and ammonoids. Fossil Record, 17: 41-57.
Griffin, J.M., Montanez, I.P., Matthews, J.A., et al., 2015. A refine protocol for delta O-18 (PO4) analysis of conodont bioapatite. Chemical Geology, 417: 11-20.
Goudemand, N., Orchard, M.J., Tafforeau, P., Urdy, S., Brühwiler, T., Brayard, A., Galfetti, T. and Bucher, H., 2012. Early Triassic conodont clusters from South China: revision of the architecture of the 15 element apparatuses of the superfamily Gondolelloidea. Palaeontology, 55: 1021-1034.
Gruszczynski, M., Hoffman, A., Malkowski, K., Veizer, J. 1992. Seawater strontium isotopic perturbation at Permian-Triassic boundary, west Spitsbergen and its implications for the interpretation of strontium isotope data. Geology, 20: 779-82.
Hallam, A., Wignal, P.B. 1997. Mass extinctions and their aftermath. Oxford University Press.
Hartmann, D.L., Klein Tank, A.M.G. Rusticucci, M., Alexander, L.V., Brönnimann, S., Charabi, Y., Dentener, F.J., Dlugokencky, E.J., Easterling, D.R., Kaplan, A., Soden, B.J., Thorne, P.W.. Wild, M. and Zhai, P.M., 2013: Observations: Atmosphere and Surface. In: Climate Change 2013: The Physical Science Basis. Contribution of Working Group I to the Fifth Assessment Report of the Intergovernmental Panel on Climate Change [Stocker, T.F., D. Qin, G.-K. Plattner, M. Tignor, S.K. Allen, J. Boschung, A. Nauels, Y. Xia, V. Bex and P.M. Midgley (eds.)]. Cambridge University Press, Cambridge, United Kingdom and New York, NY, USA.
Henderson, C.M. and Baud, A., 1996. Correlation of the Permian-Triassic boundary in Arctic Canada and comparison with Meishan, China. Proceedings of the 30th International Geological Congress (Beijing), 11: 143-152.
Henderson, C.M., Golding, M.L. and Orchard, M.J., 2018. Conodont sequence biostratigraphy of the Lower Triassic Montney Formation. Bulletin of Canadian Petroleum Geology, 66:7-22.
Henderson, C. M., Mei, S. L., 2007. Geographical Clines in Permian and Lower Triassic Gondolellids and Its Role in Taxonomy. Palaeoworld, 16: 190–201
Hinojosa, J.L., Brown, S. T., Chen, J., et al., 2012. Evidence for end-Permian ocean acidification from calcium isotopes in biogenic apatite. Geology, 40: 743-746.
Hosler, W.T., Magaritz, M., 1987. Events near the Permian- Triassic boundary. Modern Geology, 11: 155-180.
Huang, J. Y., Zhang, K. X., Zhang, Q. Y., Lu, T., Zhou, C. Y., Bai, J. K. and Hu, S. X., 2010. Discovery of Middle Triassic conodont clusters from Luoping Fauna, Yunnan Province. Earth Science—Journal of

China University of Geosciences, 35: 512-514. (In Chinese with English summary).
Huang, J.Y., Hu, S.X., Zhang, Q.Y., Donoghue, P. C.J., Benton, M.J., Zhou, C.Y., Martí nez-Pé rez, C., Wen, W., Xie, T., Chen, Z.Q., Luo, M., Yao, H.Z. and Zhang, K.X. 2018, Gondolelloid multielement conodont apparatus (*Nicorella*) from the Middle Triassic of Yunnan Province, southernwestern China. Palaeogeography, Palaeoclimatology, Palaeoecology, https:/doi.org/10.1016/j. palaeo. 2018.07.015
Huckriede, R. 1958: Die Conodonten der Mediterranen Trias und ihr stratigraphischer Wert. Paläontologische Zeitschrift 32: 141–175.
Isozaki, Y., Yao, J.X., Matsuda, T;Sakai, H., Ji, Z. S., Shimizu, N., Kobayashi, N., Kawahata, H., Nishi, H., Takano, M., Kubo, T., 2004. Stratigraphy of the Middle-Upper Permian and Lowermost Triassic at Chaotian, Sichuan, China - Record of late permian double mass extinction event. Proceedings of the Japan Academy series B-Physical and Biological Sciences, 80: 10-16.
Jiang, H.S., Lai, X.L., Luo, G.M., Aldridge, R.J., Zhang, K.X., Wignall, P.B., 2007. Restudy of conodont zonation and evolution across the P/T Boundary at Meishan Section, Changxing, Zhejiang, China. Global and Planetary.Change, 55: 39–55.
Jiang, H.S., Aldridge, R.J., Lai, X.L., Sun, Y.D. and Luo, G.M., 2008. Observations on the surface microreticulation of platform elements of *Neogondolella* (Conodonta) from the Upper Permian, Meishan, China. Lethaia, 41: 263-274.
Jiang, H. S., Aldridge, R. J., Lai, X. L., et al., 2011a. Phylogeny of the Conodont Genera *Hindeodus* and *Isarcicella* across the Permian–Triassic Boundary. Lethaia, 44: 374–382.
Jiang, H. S., Lai, X. L., Yan, C. B., et al., 2011b. Revised Conodont Zonation and Conodont Evolution across the Permian–Triassic Boundary at the Shangsi Section, Guangyuan, Sichuan, South China. Global and Planetary Change, 77: 103–115.
Jiang, H.S. and Lai, X.L., 2013. The cladistic analysis of gondolelloids and its implications. In Albanesi G.L. and G. Ortega (Eds) Conodonts from the Andes-Publicación Especial No 13-Julio 2013-Paleontological Note. Abstract: 142.
Jiang, H.S., Lai, X.L., Sun, Y.D., Wignall, P.B., Liu, J.B., Yan, C.B., 2014. Permian–Triassic conodonts from Dajiang (Guizhou, South China) and their implication for the age of microbialite deposition in the aftermath of the end-Permian mass extinction. Journal of Earth Science, 25: 413–430.
Jiang. H.S., Joachimski, M.M., Wignall, P.B., Zhang, M.H., Lai, X.L., 2015. A delayed end-Permian extinction in deepwater locations and its relationship to temperature trends (Bianyang, Guizhou Province, South China). Palaeogeography, Palaeoclimatology, Palaeoecology, 440: 690-695.
Jiang, H.S., Wignall, P.B., Chen, Z.Q., Xie, S.C., Lai, X.L., Song, H.J., Wang, L.N., 2017. Comment on "Quantitative biochronology of the Permian–Triassic boundary in South China based on conodont unitary associations" by Brosse et al.. Earth-Science Reviews, 164: 257-258.
Jin, Y.G., Wang, Y., Wang, W., Shang, Q.H., Cao, C.Q., Erwin, D.H., 2000. Pattern of marine mass extinction near the Permian–Triassic boundary in south China. Science, 289: 432–443.
Ji, Z., Yao, J., Isozaki, Y., Matsuda, T. and Wu, G., 2007, Conodont biostratigraphy across the Permian–Triassic boundary at Chaotian, in northern Sichuan, China. Palaeogeography, Palaeoclimatology, Palaeoecology, 252: 39–55.
Joachimski, M.M., Breisig, S., Buggisch, W., Talent,J.A., Mawson, R., Gereke, M., Morrow, J.M.,Day, J., and Weddige, K., 2009, Devonian climate and reef evolution: Insights from oxygen isotopes in apatite. Earth and Planetary Science Letters, 284: 599–609,
Joachimski, M.M., Lai, X.L., Shen, S.Z., Jiang, H.S., Luo, G.M., Chen, B., Sun, Y.D., 2012. Climate warming in the latest Permian and Permian–Triassic mass extinction. Geology, 40: 195–198.
Joachimski, M.M., Breisig, S., Buggisch, W., Talent,J.A., Mawson, R., Gereke, M., Morrow, J.M.,Day, J., and Weddige, K., 2009, Devonian climateand reef evolution: Insights from oxygenisotopes in apatite: Earth and Planetary Science, 284: 599–609,
Katvala, E. C., Henderson, C. M. 2012. Chemical element distributions within conodont elements and their functional implications. Paleobiology, 38: 447-458
Koike, T., Yamakita, S. and Kadota, N., 2004: A natural assemblage of *Ellisonia* sp. cf. *E. triassica* Müller (Vertebrata: Conodonta) from the uppermost Permian in the Suzuka Mountains, central Japan. Paleontological Research, 8: 241–253.
Koike, T., 2016. Multielement Conodont Apparatuses of the Ellisonidae from Japan. Paleontological Research, 20,161-175.
Kolar-Jurkovsek, T. Jurkovsek, B., Aljinovic, D., 2011. Conodont biostratigraphy and lithostratigraphy across the Permian-Triassic Boundary at the Lukac section in western Slovenia. Rivista Italiana Paleontologia E Stratigrafia, 117: 115-133.

565 Kozur, H., 1989: Significance of events in conodont evolution for the Permian and Triassic stratigraphy.
566 Courier Forschungsinstitut Senckenberg, 117: 385–408.
567 Kozur, H., 1996: The conodonts *Hindeodus*, *Isarcicella* and *Sweetohindeodus* in the Uppermost Permian
568 and Lowermost Triassic. Geologia Croatica, 49: 81–115.
569 Kozur, H., 2007. Biostratigraphy and Event Stratigraphy in Iran around the Permian–Triassic Boundary
570 (PTB): Implications for the Causes of the PTB Biotic Crisis. Global and Planetary Change, 55: 155–
571 176
572 Kozur, H., Mostler, H. & Rahimi–Yazd, A. 1975: Beiträge zur Mikropaläontologie permotriadischer
573 Schichtfolgen. Teil II: Neue Conodonten aus dem Oberperm und der basalen Trias von Nord–und
574 Zentraliran. Geologisch–Paläontologische Mitteilungen Innsbruck 5: 1–23.
575 Kozur, H. & Pjatakova, M. 1976: Die Conodontenart *Anchignathodus parvus* n.sp., eine wichtige Leiform
576 der basalen Trias. Proceedings Koninkl Nederland Akademie van Wetenschappen, Series B, 79:
577 123–128.
578 Krystyn, L., Baud, A., Richoz, S., et al., 2003. A Unique Permian–Triassic Boundary Section from the
579 Neotethyan Hawasina Basin, Central Oman Mountains. Palaeogeography, Palaeoclimatology,
580 Palaeoecology, 191: 329–344.
581 Lai, X.L., Ding, M.H. & Zhang, K.X. 1995. The significance of the discovery of Isarcicella isarcica at the
582 Meishan Permian–Triassic boundary–candidate stratotype section in Changxing, Zhejiang province.
583 Exploration of Geosciences 11, 7–11 (In Chinese with English summary).
584 Lai, X.L. 1998: Discussion on Permian–Triassic conodont study. Permophiles, 31: 32–35.
585 Lai, X.L., Wignall, P.B., Zhang, K.X., 2001. Palaeoecology of the conodonts *Hindeodus* and *Clarkina*
586 during the Permian–Triassic transitional period. Palaeogeography, Palaeoclimatology, Palaeoecology
587 171: 63–72.
588 Le Houedec, S., McCulloch, M., Trotter, J. et al., 2017. Conodont apatite 87Sr/86Sr and 44Ca/40Ca
589 compositions and the implications for the evolution of Palaeozoic to early Mesozoic weawater.
590 Chemical Geology, 453: 55-65.
591 Li, Z.S., Zhan, L.P., Dai, J.Y., Jin, R.G., Zhu, X.F., Zhang, J.H., Huang, H.Q., Xu, D.Y., Yan, Z. & Li,
592 H.M. 1989: Study on the Permian–Triassic biostratigraphy and event stratigraphy of northern
593 Sichuan and southern Shaanxi. Geological Memoirs, Series, vol. 29. Geological Publishing House,
594 Beijing. 435 pp (In Chinese with English summary).
595 Li, Y., Zhao, L.S., Chen, Z.Q., Cao, L., Wang, X. D., 2012. Oceanic environmental changes on a shallow
596 carbonate platform (Yangou, Jiangxi Province, South China) during the Permian-Triassic transition:
597 Evidence from rare earth elements in conodont bioapatite. Palaeogeography, Palaeoclimatology,
598 Palaeoecology, 486: 6-16.
599 Liang, L., Tong, J.N., Song, H.J., Song, T., Tian, L., Song, H.Y., Qiu, H.O., 2016. Lower-Middle Triassic
600 conodont biostratigraphy of the Mingtang section, Nanpanjiang Basin, South China. Palaeogeography,
601 Palaeoclimatology, Palaeoecology, 459, 381–393.
602 Luo, G. Lai, X., Feng, Q., Jiang, H., Wignall, P. B., Zhang, K., Sun, Y., Wu, J., 2008, End-Permian
603 conodont fauna from Dongpan section: Correlation between the deep and shallow-water facies. Science
604 in China (D), 51:11–1622.
605 Martin, E.E., Macdougall, J.D. 1995. Sr and Nd isotopes at the Permian/Triassic boundary: a record of
606 climate change. Chemical Geology, 125: 73-100.
607 Mei, S.L., Zhang, K.X., Wardlaw, B.R., 1998. A refined zonation of Changhsingian and Griesbachian
608 neogondolellid conodonts from the Meishan Section, candidate of the global stratotype section and
609 point of the Permian–Triassic Boundary. Palaeogeography, Palaeoclimatology, Palaeoecology 143:
610 213–226.
611 Mei, S.L., Henderson, C.M, Cao, C.Q., 2004. Conodont sample-population approach to defining the base
612 of the Changhsingian Stage, Lopingian Series, Upper Permian. Palynology and Micropalaeontology of
613 Boundaries, Geological Society Special Publication 230: 105-121.
614 Mei, S.L., Zhang, K.X., Wardlaw, B.R., 1998. A refined zonation of Changhsingian and Griesbachian
615 neogondolellid conodonts from the Meishan Section, candidate of the global stratotype section and
616 point of the Permian–Triassic Boundary. Palaeogeography, Palaeoclimatology, Palaeoecology, 143:
617 213–226.
618 Metcalfe, I., 2012. Changhsingian (Late Permian) conodonts from Son La, northwest Vietnam and their
619 stratigraphic and tectonic implications. Journal of Asian Earth Sciences, 50: 141-149.
620 Metcalfe, I., Nicoll, R. S. 2007. Conodont biostratigraphic control on transitional marine to non-
621 marine Permian-Triassic boundary sequences in Yunnan-Guizhou, China. Palaeogeography,

622 Palaeoclimatology, Palaeoecology, 252: 56–65.
623 Mine, A.H., Waldeck, A., Olack, G., Hoerner, M.E., Alex, S., Colman, A.S., 2017. Microprecipitation and
624 delta O-18 analysis of phosphate for palaeoclimate and biogeochemistry research. Chemical Geology,
625 460: 1-14.
626 Nicoll, R.S., Metcafle, I., Wang, C., 2002, New species of the conodont genus *Hindeodus* and conodont
627 biostratigraphy of the Permian–Triassic boundary interval. Journal of Asian Earth Science, 20: 609–631.
628 Orchard, M.J., Nassichuk, W.W., Rui, L., 1994. Conodonts from the Lower Griesbachian *Otoceras*
629 latilobatum bed of Selong, Tibet and the position of the Permian–Triassic boundary. Canadian Society
630 of Petroleum Geologists. Proc. Pangea Confernce, Memoir, 17: 823–843.
631 Orchard, M.J., Krystyn, L., 1998.Conodonts of the lowermost Triassic of Spiti, and new zonation based
632 onNeogondolella successions. Rivista Italiana di Paleontogia e Stratigrafia, 104: 341–368.
633 Orchard, M.J., Struik, L.C., and Taylor, H., 1998: New conodont data from the Cache Creek Group,
634 central British Columbia; in Current Research 1998-A; Geological Survey of Canada, p. 99-105.
635 Orchard, M. J. and Rieber, H., 1999. Multielement *Neogondolella* (Conodonta, Upper Permian-Middle
636 Triassic). Bollettino della Società Paleontologica Italiana, 37: 475–488.
637 Orchard, M. J., 2005. Multielement conodont apparatuses of Triassic Gondolellidea. Special Papers in
638 Palaeontology, 73: 73–101.
639 Orchard, M. J., 2007. Conodont diversity and evolution through the latest Permian and Early Triassic
640 upheavals. Palaeogeography, Palaeoclimatology, Palaeoecology, 252: 93-117.
641 Payne, J.L., Clapham, M.E. 2012. End-Permian Mass Extinction in the Oceans: An Ancient Analog for the
642 Twenty-First Century? Aanual Review of Earth and Planetary Scienses, 40: 89-111.
643 Perri, M. C., Farabegoli, E., 2003. Conodonts across the Permian–Triassic Boundary in the Southern Alps.
644 Courier Forschung Institute of Senckenberg, 245: 281–313.
645 Perri, M.C., Molloy, P.D.,Talent, J.A., 2004. Earliest Triassic conodonts from Chitral, northernmost
646 Pakistan. Rivista Italiana Di Paleontologia E Stratigraphia, 110: 467-478.
647 Purnell, M.A., Jones, D. 2012. Quantitative analysis of conodont tooth wear and damage as a test of
648 ecological and functional hypothesis. Paleobiology, 38: 605-626.
649 Purnell, M.A., Zhang, M.H., Jiang, H.S., Lai, X.L., 2018. Reconstruction, composition and homology of
650 conodont skeletons: a response to Agematsu *et al*.. Palaeontology, 61(5): 793–796. https:
651 //doi.org/10.1111/pala.12387
652 Quinton, P.C., Leslie, S.A., Herrmann, A.D., MacLeod, K. G., 2016. Effects of extraction protocols on the
653 oxygen isotope composition of conodont elements. Chemical Geology, 431: 36-43.
654 Romano, C., Goudemand, N., Vennemann, T. W., Ware, D., Scheneebeli-Hermann, E., Hochuli, P. A.,
655 Brühwiler, T., Brinkmann, W., Bucher, H., 2013. Climatic and biotic upheavals following the end-
656 Permian mass extinction. Nature Geoscience, 6: 57-60.
657 Schaal, E.K., Clapham, M. E., Rego, B. L., Wang, S. C., Payne, J. L., 2016. Comparative size evolution of
658 marine clades from the Late Permian through Middle Triassic. Paleobiology, 42: 127-142.
659 Schobben, M., Joachimski, M.M., Korn, D., Leda, L., Korte, C., 2014. Palaeotethys seawater temperature
660 rise and an intensified hydrological cycle following the end-Permian mass extinction. Gondwana
661 Research, 26: 675-683.
662 Shen, S.Z., James, L., Crowley, J.L., Wang, Y., Bowring, S.A., Erwin, D.H., Sadler, P.M., Cao, C.Q.,
663 Rothman, D.H., Henderson, C.M., Ramezani, J., Zhang, H., Shen, Y.A., Wang, X.D., Wang, W., Mu,
664 L., Li, W.Z., Tang, Y.G., Liu, X.L., Liu, L.J., Zeng, Y., Jiang, Y.F., Jin, Y.G., 2011. Calibrating the
665 End-Permian mass extinction. Science, 334: 1367–1372.
666 Song, H.J, Wignall, P. B, Tong, J N., Bond, D. P.G., Song, H. Y., Lai X.L., Zhang,K.X., Wang, H.M,.
667 Chen, Y. L. 2012. Geochemical evidence from bio-apatite from multiple oceanic anoxic events during
668 the Permian-Triassic transition and the link with the end-Permian mass extinction and recovery. Earth
669 and Planetary Science Letters, 353: 12-21.
670 Song, H.J., Wignall, P.B., Tong, J.N., Yin, H.F., 2013. Two pulses of extinction during the Permian–
671 Triassic crisis. Nature Geoscience. 6: 52–56.
672 Song, H.J., Wignall, P B., Tong, J.N., Song H.Y., Chen J., Chu D.L., Tian L., Luo M., Zong K.Q., Chen
673 Y.L., Lai X.L., Zhang K.X., Wang H.M., 2015. Integrated Sr isotope variations and global
674 environmental changes through the Late Permian to early Late Triassic. Earth and Planetary Science
675 Letters, 424: 140-147.
676 Sudar, M., Jovanovic, D., Kolar-Jurkovsek, T., 2007. Late Permian conodonts from Jadar Block (Vardar
677 Zone, northwestern Serbia). Geologica Carpathica, 58: 145-152.
678 Sudar, M.; Perr, M. C., Haas, J., 2008. Conodonts across the Permian-Triassic boundary in the Bukk

679 Mountains (NE Hungary). Geologica Carpathica, 59: 491-502.
680 Sun, D.Y, Tong, J.N, Xiong, Y., Tian, L. and Yin, H.F, 2012, Conodont biostratigraphy and evolution
681 across Permian–Triassic boundary at Yangou Section, Leping, Jiangxi Province, South China. Journal
682 of Earth Science, 23: 311–325.
683 Sun, Y.D,, Joachimski, M, M., Wignall, P.B,, Yan, C.B,, Chen,Y.L,, Jiang, H.S,, Wang, L.N,, Lai, X.L.
684 2012. Lethally Hot Temperatures during the Early Triassic Greenhouse. Science，338: 366-370.
685 Sun, Y.D., Wiedenbeck, M., Joachimski, M.M., et al., 2016. Chemical and oxygen composition of gem-
686 quality apatites: implications for oxygen isotope reference materials for secondary ion mass
687 spectrometry(SIMS). Chemical Geology, 440: 164-178.
688 Twitchett, R. J., 2005. The lilliput effect in the aftermath of end-Permian extinction event. Albertiana, 33:
689 79-81.
690 Trotter, J.A., Williams, I.S., Nicora, A., Mazza, M., Rigo, M., 2015. Long-term cycles of Triassic climate
691 change: a new δ18O record from conodont apatite. Earth and Planetary Science Letters. 415: 165-174.
692 Urbanek, A., 1993. Biotic crises in the history of Upper Silurian graptoloids: a palaeobiological model.
693 Historical Biology, 7: 29-50.
694 Wang, C.Y., 1994. A conodont based high-resolution eventostratigraphy and biostratigraphy for the
695 Permian–Triassic boundaries in South China. Palaeoworld, 4, 234–248.
696 Wang, C.Y., 1995a. Conodonts of Permian–Triassic boundary beds and stratigraphic boundary. Acta
697 Palaeontologica Sinica, 34 (2): 129–151 (in Chinese with English abstract).
698 Wang, C.Y., 1995b. Conodonts of Permian–Triassic boundary beds and biostratigraphic boundary in
699 Zhongxin Dadui section, Changxing, Zhejiang. Chinese Science Bulletin 40 (8), 719–722
700 Wang, C.Y., 1996. Conodont evolutionary lineage and zonation for the Latest Permian and the Earliest
701 Triassic. Permophiles,29: 30–37.
702 Wang, C.Y., Wang, Z.H., 1981. Permian conodonts from Longtan Formation and Changhsing Formation
703 of Changxing, Zhejiang and their stratigraphical and palaeoecological significance. Selected Papers on
704 the 1st Convention of Micropalaeontological Society of China. Science Press, Beijing, pp. 114–120 (in
705 Chinese with English abstract).
706 Wang, G.Q., Xia, W.C. 2003. The Changhsingian conodont zonation and variation of organic carbon
707 isotope of Huangshi Ermen section, Hubei Province. Geoscience, 17: 378-386.
708 Wang, G.Q., Xia, W.C., 2004. Conodont zonation across the Permian-Triassic boundary at the Xiakou
709 section, Yichang city, Hubei Province and its correlation with the Global Stratotype Section and Point
710 of the PTB. Canadian Journal of Earth Sciences, 41: 323-330.
711 Wang, L.N., Wignall, P. B., Wang, Y.B Jiang, H.S., Sun, Y.D., ,Li, G.S., Yuan, J.L., Lai, X.L, 2016.
712 Depositional conditions and revised age of the Permo-Triassic microbialites at Gaohua section, Cili
713 County (Hunan Province, South China), Palaeogeography, Palaeoclimatology, Palaeoecology, 443:
714 156-166.
715 Wang, L.N., Wignall, P.B., Sun, Y.D.,Yan, C. B.,, Zhang, Z.T., Lai, X.L., 2017. New Permian-Triassic
716 conodont data from Selong (Tibet) and the youngest occurrence of Vjalovoganthus. Journal of Asian
717 Earth Science, 146: 152-167.
718 Wardlaw, B.R., Nestell, M.K., Nestell, G. P. Elwood, B. B., Lan, L. P. L., 2015. Conodont biostratigraphy
719 of the Permian-Triassic boundary sequence at Lung Cam, Vietnam. Micropaleontology, 61: 313-334.
720 Wu, G.C., Ji, Z.S., Trotter, J.A., Ji, Z. S., Zhou, L. Q., 2014. Conodont biostratigraphy of a new Permo-
721 Triassic boundary section at Wenbudangsang, north Tibet. Palaeogeography, Palaeoclimatology,
722 Palaeoecology, 411: 188-207.
723 Wu, G.C., Yao, J.X., Ji, Z.S. 2003. Conodont Fauna of late Upper Permian in Xinfeng Area Jiangxi
724 Province. Acta Scientiarum Naturalium Universitatis Pekinensis, 39: 211-218
725 Wu, G.C., Yao, J.X., Ji, Z.S. 2002. Conodont Fauna of Late Permian to Early Triassic in Leping Area,
726 Jiangxi Province. Acta Scientiarum Naturalium Universitatis Pekinensis, 38: 790-795.
727 Xie, S.C., Pancost, R.D., Yin, H.F., Wang, H.M., Evershed, R.P., 2005. Two episodes of microbial change
728 coupled with Permo/Triassic faunal mass extinction. Nature, 434:494–497.
729 Yang, B., Lai, X., Wignall, P. B., Jiang, H., Yan, C., Sun, Y., 2012, A newly discovered earliest Triassic
730 chert at Gaimao section, Guizhou, Southwestern China. Palaeogeography, Palaeoclimatology,
731 Palaeoecology, 344-345: 69–77.
732 Yan, C.B., Wang, L.N., Jiang, H.S., Wignall, P.B., Sun, Y.D., Chen, Y.L., Lai, X.L., 2013. Uppermost
733 Permian to Lower Triassic conodonts at Bianyang section, Guizhou, South China. Palaios, 28: 509–522.
734 Yin, H.F., Yang, F.Q., Zhang, K.X.,Yang, W.P., 1988. A proposal to the biostratigraphy criterion of
735 Permian/ Triassic boundary. Memoire della Societa de Geologic Italiana, 34: 329- 344.

Yin, H.F., Zhang, K.X., Tong, J.N., Yang, Z.Y., Wu, S.B., 2001. The Global Stratotype Section and Point (GSSP) of the Permian–Triassic Boundary. Episodes, 24: 102–114.

Yin, H.F., Feng, Q.L., Lai, X.L., Baud, A., Tong, J.N., 2007. The protracted Permo-Triassic crisis and the multi-act mass extinction around the Permian–Triassic boundary. Global and Planetary Change, 55: 1–20.

Yin, H.F., Jiang, H.S., Xia, W.C., Feng, Q.L., Zhang, N., Shen, J., 2014. The end-Permian regression in South China and its implication on mass extinction. Earth Science Reviews, 137: 19–33.

Yousefirad, M., Ghanbari, S., Shirazi, M/P., 2013. Using conodont elements to distinguish Permian-Triassic boundary disconformity near Haftad Gholleh, central Iran. Earth Science Research Journal, 17: 61-65.

Yuan, D.X., Shen, S.Z., Henderson, C.M., Chen, J., Zhang, H., Feng, H.Z., 2014. Revised conodont-based integrated high-resolution timescale for the Changhsingian Stage and end-Permian extinction interval at the Meishan sections, South China. Lithos, 204: 220–245.

Yuan, D.X., Chen, J., Zhang, Y.C., Zheng, Q. F., Shen, S.Z. 2015. Changhsingian conodont succession and the end-Permian mass extinction event at the Daijiagou section in Chongqing, Southwest China. Journal of Asian Earth Sci, 105: 234-251.

Yuan, D. X., Zhang, Y. C., Shen, S. Z., 2018. Conodont succession and reassessment of major events around the Permian-Triassic boundary at the Selong Xishan section, southern Tibet, China. Global and Planetary Change, 161: 194-210.

Yuan, D. X., Shen,S. Z., 2011. Conodont succession across the Permian-Triassic Boundary of the Liangfengya section, Chongqing, South China. Acta Palaeontologica Sinica, 50: 420-438.

Zhang, K.X., 1984. The news of conodont fauna from "*Otoceras*" bed at Baoqin section of Changxing, Zhejiang. Earth Sciences —Journal of China University of Geosciences, 3: 104 (in Chinese with English abstract).

Zhang, K.X., 1987. The Permian–Triassic conodont fauna in Changxing area, Zhejiang province and its stratigraphic significance. Earth Sciences—Journal of China University of Geosciences, 12: 193–200. (in Chinese with English abstract).

Zhang, K.X., Lai, X.L., Ding, M.H., Wu, S.B., Liu, J.H., 1995. Conodont sequence and its global correlation of P/T Boundary in Meishan section, Changxing, Zhejiang province. Earth Sciences–Journal of China University of Geosciences, 20: 669–678 (in Chinese with English abstract).

Zhang, K.X., Lai, X.L., Tong, J.N., Jiang, H.S., 2009. Progresses on study of conodont sequence for the GSSP section at Meishan, Changxing, Zhejiang Province, South China. Acta Palaeontologica Sinica, 48, 474–486 (in Chinese with English abstract).

Zhang, K. X., Tong, J.N., Shi, G.R,, Lai, X.L., Yu, J.X., He, W.H., Peng, Y.Q., Jin, Y.L. 2007, Early Triassic conodont-palynological biostratigraphy of the Meishan D Section in Changxing, Zhejiang Province, South China. Palaeogeography, Palaeoclimatology, Palaeoecology, 252: 4–23.

Zhang, N., Jiang, H.S., Zhong, W.L., Huang, H.H., Xia, W.C., 2014. Conodont Biostratigraphy across the Permian-Triassic Boundary at the Xinmin Section, Guizhou, South China. Journal of Earth Science, 25: 779–786.

Zhang, Y., Zhang, K. X., Shi, G. R., He, W. H., Yuan, D. X., Yue, M. L., Yang, T. L., 2014. Restudy of conodont biostratigraphy of the Permian–Triassic boundary section in Zhongzhai, southwestern Guizhou Province, South China. Journal Asian Earth Science, 80: 75-83.

Zhang, M.H., Jiang, H.S., Purnell, M.A., Lai, X.L. 2017. Testing hypotheses of element loss and instability in the apparatus composition of complex conodonts: articulated skeletons of *Hindeodus*. Palaeontology, 60: 595–608.

Zhang, L., Orchard, M.J., Algeo, T.J., Chen, Z.-Q., Lyu, Z., Zhao, L., Kaiho, K., Ma, B. and Liu, S., 2017. An intercalibrated Triassic conodont succession and carbonate carbon isotope profile, Kamura, Japan. Palaeogeography, Palaeoclimatology, Palaeoecology doi:10.1016/j.palaeo.2017.09.001

Zhao, L.S., Orchard, M. J., Tong, J.N., Sun, Z.Y., Zuo, J.X., Zhang, S. and Yuan A., 2007, Lower Triassic conodont sequence in Chaohu, Anhui Province, China and its global correlation. Palaeogeography, Palaeoclimatology, Palaeoecology, 252: 24–38.

Zhao, L.S., Wu, Y.B., Hu, Z.C., Zhou, L., Liu, Y. S., Shi, Y. F., Zhang, S. X., Tong, J. N., Yuan, P., 2009. Trace Element Compositions in Conodont Phosphates Responses to Biotic Extinction Event: A Case Study for Main Act of Global Boundary Stratotype Section and Point of the Permian-Triassic. Earth Science—Journal of China University of Geosciences, 34: 725-732.

Zhao, L.S., Chen, Z. Q., Algeo, T.J., Chen, J. B., Chen, Y. L., Tong, J. N., Gao, S., Zhou, L., Hu, Z. C., Liu, Y. S., 2013. Rare-earth element patterns in conodont albid crowns: Evidence for massive inputs of

volcanic ash during the latest Permian biocrisis? Global and Planetary Change, 150: 135-151.
Zhao, L.S., Chen, Y.L., Chen, Z.Q., Cao, L., 2013. Uppermost Permian to Lower Triassic conodont zonation from Three Gorges area, South China. Palaios, 28: 523-540.
Zhou, L.Q., Williams, I. S., Liu, J. H., Ji, Z.S., Xiao, Y.F., Liu, D.Y., 2012. Methodology of SHRIMP in-Situ O isotopes analysis on Conodont. Acta Geologica Sinica, 86: 611-618.

Figure Captions

Fig. 1 Key conodont species across the PTB picked from numerous sections in South China.
All are P_1 elements. Scale bar equals 200 μm.
1. *Clarkina planata* (Clark, 1959), reprint from Chen et al. (2015), Fig.6, 1.
2. *Hindeodus sosioensis* Kozur, 1996, reprint from Jiang et al. (2014), pl.3, 10.
3. *Hindeodus praeparvus* Kozur, 1996, reprint from Jiang et al. (2007), pl. IV, 36.
4. *Clarkina krystyni* (Orchard & Krystyn, 1998), reprint from Chen et al. (2015), Fig.6, 2.
5. *Hindeodus latidentatus* (Kozur, Mostler and Rahimi-Yazd, 1975), reprint from Jiang et al. (2007), pl. IV, 3.
6. *Hindeodus changxingensis* Wang, 1995, reprint from Jiang et al. (2007), pl. IV, 21.
7. *Hindeodus parvus* (Kouzr & Pjatakova, 1976), reprint from Jiang et al. (2011), pl.1, fig.9.
8. *Isarcicella lobata* Perri & Farabegoli, 2003, reprint from Jiang et al. (2011), pl.3, fig.4.
9. *Isarcicella staeschei* Dai & Zhang, 1989 (in Li et al., 1989), reprint from Jiang et al. (2011), pl.3, fig.12.
10. *Isarcicella isarcica* (Huckriede, 1958), reprint from Jiang et al. (2011), pl.2, fig.9.
11. *Neoclarkina discreta* (Orchard & Krystyn, 1998), reprint from Chen et al. (2015), Fig.6, 14.
12. *Clarkina changxingensis* (Wang & Wang, 1981), reprint from Jiang et al. (2007), pl. I, 13.
13. *Clarkina meishanensis* Zhang et al., 1995, reprint from Jiang et al. (2011), pl.4, fig.9.
14. *Clarkina taylorae* (Orchard, 1994), reprint from Jiang et al. (2011), pl.5, fig.6, bed 29d.
15. *Clarkina yini* (Mei et al., 1998), reprint from Jiang et al. (2011), pl.5, fig.10, bed 26.

Fig. 2 Tethys conodont zones correlation across the Permian-Triassic Boundary. Conodont zonation of Meishan is summarized after Chen Z.Q. et al. (2015), Yin et al. (2014), Yuan et al. (2014), Zhang et al. (2009); the original data are from Jiang et al. (2007, 2011b) and Zhang et al. (2007). Conodont zonations of Shangsi, Dajiang and Jiarong are from Jiang et al. (2011b), Jiang et al. (2014) and Chen Y.L. et al. (2015), respectively. Conodont zonations of Spiti and South Alps are from Orchard and Krystyn (1998) and Perri and Farabegoli (2003), respectively. Conodont zonation of Iran is from Kozur (2007).

Fig. 3 Conodont zones constrain the timing of the mass extinction across the PTB. A~F, different extinction horizon or interval at Meishan from numerous references: A is from Jin et al. (2000); B is from Xie et al. (2005); C is from Yin et al. (2007); D is from Shen et al. (2011); E is from Song et al. (2013). F, extinction horizon at the Shangsi section (Jiang et al., 2015); G, extinction horizon at the Bianyang section (Jiang et al., 2015). Abbreviation of conodont zones, *H. sos. =Hindeodus sosioensis*, *I. isar. =Isarcicella isarcica*, *I. s.=Isarcicella staeschei*, *I. lob*. *= Isarcicella lobata*, *C. t = Clarkina taylorae*, *H. c = Hindeodus changxingensis*, *C. m = Clarkina meishanensis*, *C. yini= Clarkina yini*. Absolute ages are from Burgess et al. (2014). Dark grey shows the temperature trends across the PTB (Joachimski et al., 2012; Jiang et al., 2015). Light grey rectangular area shows the warming interval.

Fig. 4 Simplified Phylogeny of conodont *Hindeodus* and *Isarcicella* (after Jiang et al. 2011a)

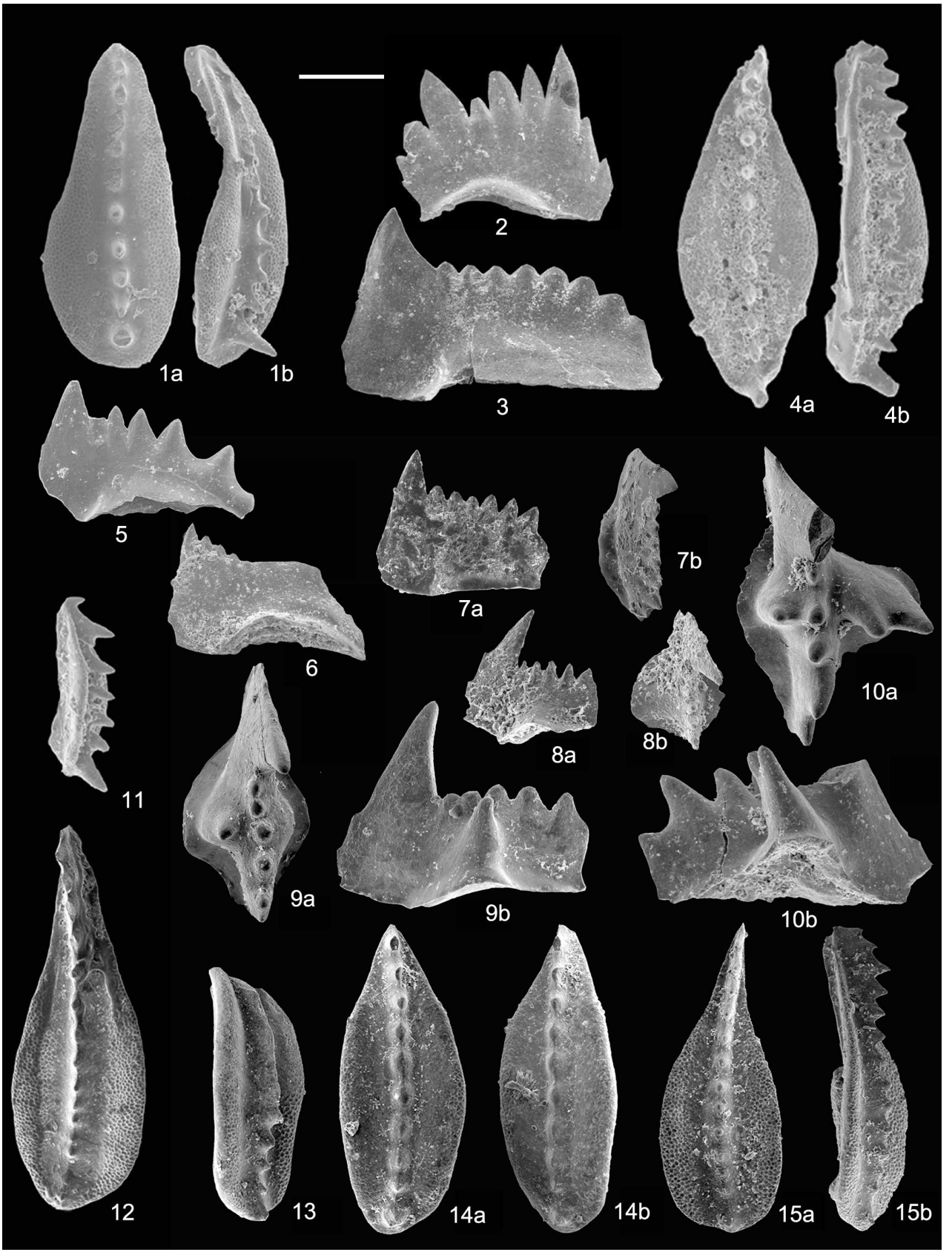
1a
1b
2
3
4a
4b
5
6
7a
7b
8a
8b
9a
9b
10a
10b
11
12
13
14a
14b
15a
15b

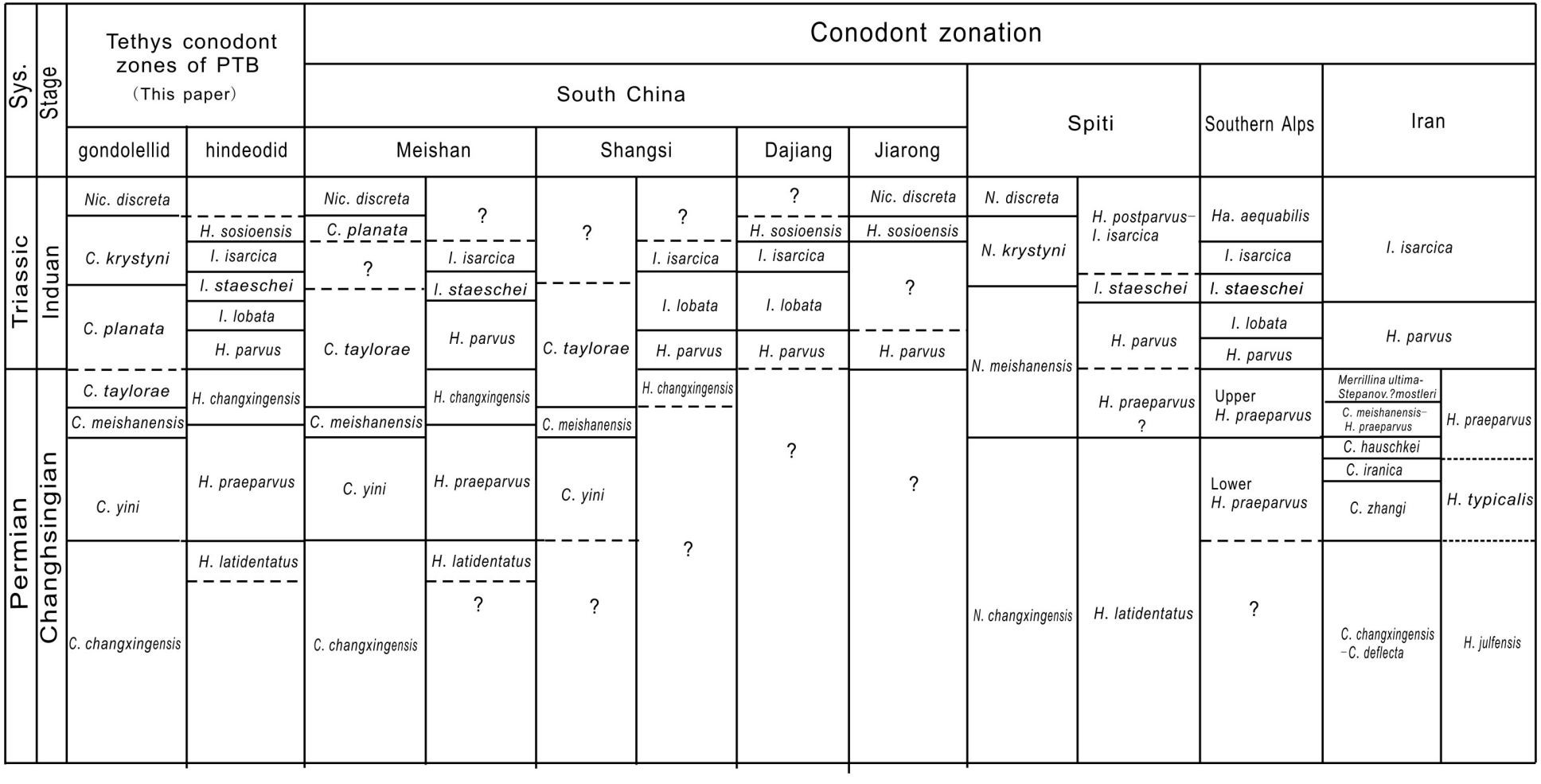
Sys.
Stage
Tethys conodont zones of PTB (This paper)
Conodont zonation
South China
Spiti
Southern Alps
Iran
gondolellid
hindeodid
Meishan
Shangsi
Dajiang
Jiarong
Triassic
Induan
Permian
Changhsingian
Nic. discreta
C. krystyni
C. planata
H. sosioensis
I. isarcica
I. staeschei
I. lobata
H. parvus
C. taylorae
C. meishanensis
C. yini
C. changxingensis
H. changxingensis
H. praeparvus
H. latidentatus
?
N. discreta
N. krystyni
N. meishanensis
N. changxingensis
H. postparvus–I. isarcica
H. praeparvus ?
Ha. aequabilis
Upper H. praeparvus
Lower H. praeparvus
Merrillina ultima-Stepanov.?mostleri
C. meishanensis–H. praeparvus
C. hauschkei
C. iranica
C. zhangi
C. changxingensis –C. deflecta
H. praeparvus
H. typicalis
H. julfensis

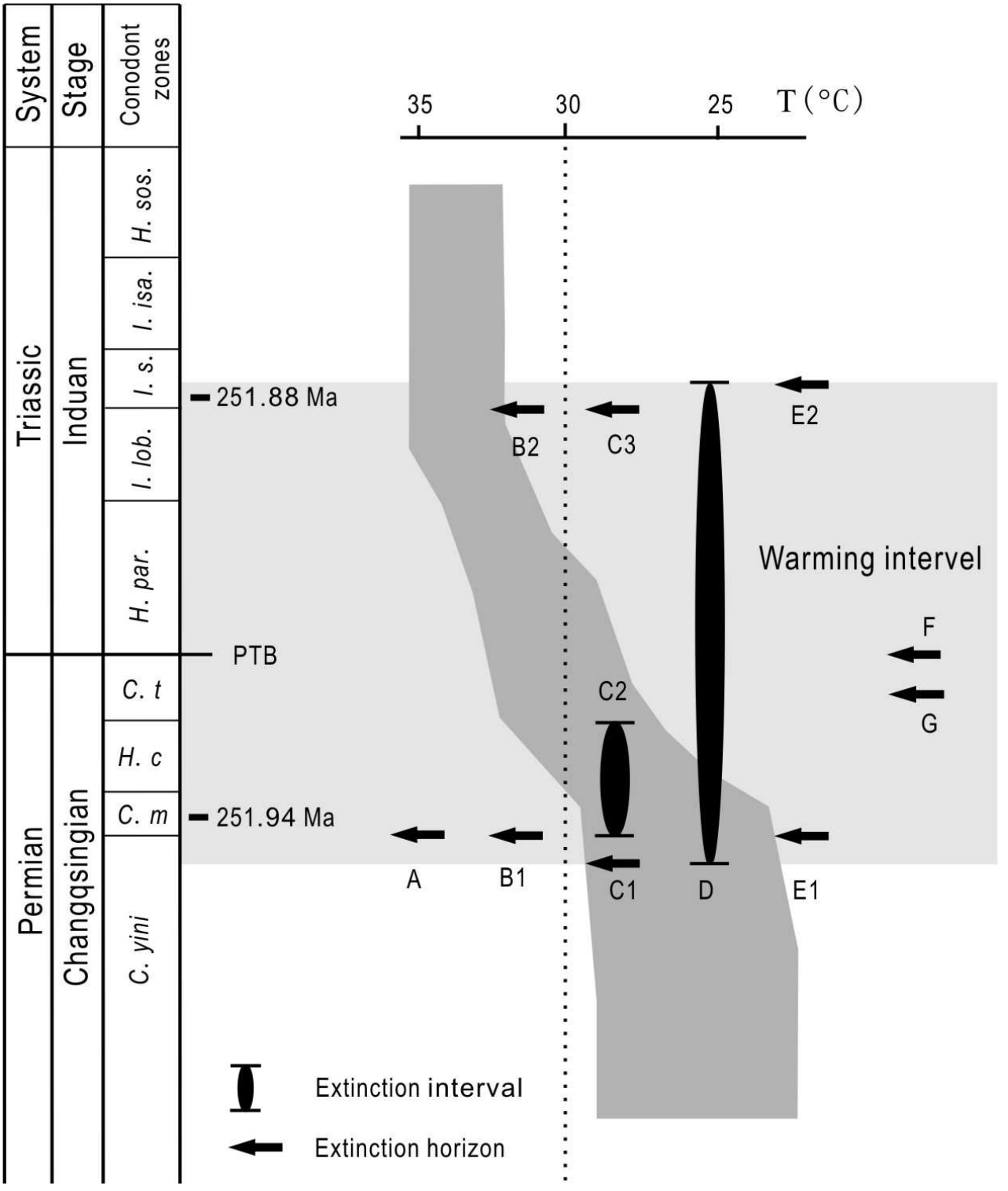
System
Stage
Conodont zones
Triassic
Induan
H. sos.
I. isa.
I. s.
I. lob.
H. par.
Permian
Changqsingian
C. t
H. c
C. m
C. yini
35
30
25
T (°C)
251.88 Ma
PTB
251.94 Ma
B2
C3
E2
Warming intervel
F
G
C2
A
B1
C1
D
E1
Extinction interval
Extinction horizon

Permian	Triassic	System
Changqsingian	Induan	Stage